Tuning Electronic Properties of Metallic Atom in Bondage to a Nanospace

Jun Tang,[†] Gengmei Xing,[†] Hui Yuan,[†] Wenbin Cao,[†] Long Jing,[†] Xingfa Gao,[†] Li Qu,[†] Yue Cheng,[†] Chang Ye,[†] Yuliang Zhao,*[,†] Zhifang Chai,[†] Kurash Ibrahim,[‡] Haijie Qian,[‡] and Run Su[‡]

Lab for Bio-Environmental Health Sciences of Nanoscale Materials, and Beijing Synchrotron Radiation Facility, Institute of High Energy Physics, The Chinese Academy of Sciences, Beijing 100049, People's Republic of China

Received: January 20, 2005; In Final Form: February 24, 2005

The possibility of modulating the electronic configurations of the innermost atoms inside a nanospace, nano sheath with chemical modification was investigated using synchrotron X-ray photoelectron spectroscopy. Systems of definite nanostructures were chosen for this study. Systematic variations in energy, intensity, and width of π^* and σ^* O 1s core level spectra, in absorption characteristics of C 1s→π^* transition, in photoabsorption of pre-edge and resonance regions of the Gd 4d→4f transition, were observed for Gd@C_{82} (an isolated nanospace for Gd), Gd@$C_{82}(OH)_{12}$ (a modified nanospace for Gd), and Gd@$C_{82}(OH)_{22}$ (a differently modified nanospace for Gd), and the reference materials Gd-DTPA (a semi-closed space for Gd) and Gd_2O_3. A sandwich-type electronic interaction along [outer modification group]−[nano sheaths]−[inner metallic atom] was observed in the molecules of modifications. This makes it possible to control electron-donation directions, either from the innermost metallic atom toward the outer nano sheaths or the reverse. The results suggest that one may effectively tune the fine structures of electronic configurations of such a metallic atom being astricted into nanostructures through changing the number or category of outer groups of chemical modifications. This may open a door to realizing the desired designs for electronic and magnetic properties of functionalized nanomaterials.

Introduction

To experimentally and theoretically investigate the unique characteristics of a definite nanospace, hollow and endohedral fullerenes with nanocages can both serve as the model systems. When metallic atoms or clusters are encapsulated into the cages (metallofullerenes),[1−4] they exhibit properties different from those not being astricted in the nanospace. The electronic properties of the metallofullerene have been studied by many techniques such as X-ray photoelectron spectroscopy (XPS),[5−11] electron spin resonance (ESR),[12−14] extended X-ray absorption fine structure (EXFAS),[15] UV−vis−NIR absorption spectra,[16,17] and synchrotron X-ray diffraction (SXRD),[18,19] etc. It has been clarified that the encaged metal in the nanospace is not "free" but has strong interaction with those carbons forming the cage. As an electron-donator, the metal atom donates its valence electrons to carbons and greatly alters the electronic configurations of the cage of fullerene. For example, the electronic interactions between La atom and the carbon cage in La@C_{82} result in a new peak at 0.64 eV below the Fermi level corresponding to a singly occupied molecular orbital (SOMO) level. While La donates three electrons to the LUMO and (LUMO+1) levels of La@C_{82},[5,6,20] the La 5p orbital considerably mixes with the lowest σ-state of C_{82}. The electronic interactions between the inner atom in the nanospace and the outer cage can largely affect the properties of the whole molecular system. For instance, it was reported that the interactions between La atom and C_{82} cage lead to the vanishing of the energy difference between isomers of C_{3v} and C_2 structures.[20] For different metal atoms, the consequence of this interaction is different. In Sc@C_{82} or Y@C_{82}, Sc or Y atom is strongly bounded to the C_{82} cage and can hardly move in the cage even at room temperature.[18,21,22] For Gd@C_{82}, one of the most important molecules in the metallofullerene family, that interaction results in a significant overlap of the electron density in the potential distribution between the Gd atom and the carbon cage.[19]

No matter how strong the interaction between the inner atom and cage is, as long as the mutual interaction exists, it provides us with the possibility to modulate the electronic property of the metal atom through different chemical modifications applied to the carbon cage. In this study, we first chemically modified the outer cage of Gd@C_{82} with a different number of hydroxyl groups to try to tune the properties of inner metal atom. After chemical purification, the changes in the electronic properties of the core Gd atom in Gd@$C_{82}(OH)_{22}$, Gd@$C_{82}(OH)_{12}$, Gd@C_{82}, Gd-DTPA, and Gd_2O_3 were investigated.

Recently, we found that neutron and X-ray were two effective means to probe the uniqueness of a nanospace, for example, fullerene cages. Neutrons, because of the electronically neutral property, were shown to be more suitable for probing the cage itself.[23] To explore the electronic properties of the metal atom inside the cage, X-ray techniques such as X-ray photoelectron spectroscopy are more powerful. It has been demonstrated that through the collection of the partial electron-yield (PEY), the unoccupied states of the selected elements in Gd@C_{82} can be identified from the fine structures of the X-ray absorption spectra.[24−27] In this paper, synchrotron radiation XPS techniques were employed to study the properties of Gd 4d, C 1s, and O

* Corresponding author. Tel./Fax: +86-10-8823-3191. E-mail: zhaoyuliang@ihep.ac.cn.
[†] Lab for Bio-Environmental Health Sciences of Nanoscale Materials.
[‡] Beijing Synchrotron Radiation Facility.

10.1021/jp050374k CCC: $30.25
Published on Web 04/02/2005

1s electrons in $Gd@C_{82}(OH)_{22}$, $Gd@C_{82}(OH)_{12}$, $Gd@C_{82}$, Gd-DTPA, and Gd_2O_3. The same metallic atom, but enclosed in different spaces, was studied in a comparative way for the first time. Through analyses of a volume of experimental data, we show how much the electronic properties of the inner metallic atom can be tuned by chemical modifications to the outer surface of the nanospace.

Experimental Section

The metallofullerenes were synthesized using the arc discharge method.[28] The soot was dissolved in DMF, and the products were extracted using a high-temperature and high-pressure method.[29,30] Separation and isolation of $Gd@C_{82}$ were performed using high performance liquid chromatography (HPLC, LC908-C60, Japan Analytical Industry Co.) coupling with 5PBB and then Buckyprep columns (Nacalai Co. Japan, 20 × 250 mm). The isolated $Gd@C_{82}$ species were identified by the matrix-assisted laser desorption time-of-flight mass spectrometer (MADLI-TOF-MS, AutoFlex, Bruker Co., Germany). The purity of the final $Gd@C_{82}$ product was about 99.9%. The synthesis method for water-soluble Gd-fullerenols was the alkaline reaction.[31,32] The $Gd@C_{82}$ toluene solution was first mixed with aqueous solution containing 50% NaOH. Several drops of catalyst of 40% TBAH (tetrabutylammonium hydroxide) were then added into the reaction system. The mixture of solutions was vigorously stirred at room temperature. The color of the solution in the beaker changed from the originally deep yellow into colorless; meanwhile, a brown sludge precipitated onto the bottom of the beaker. After adding more water into the brown sludge, it was stirred overnight. The brown precipitate was washed using MeOH and was then removed by the vacuum-evaporation system. This washing manipulation was repeated several times for a complete removal of the remnant TBAH and NaOH. The brown precipitate was dissolved into deionized water with continuous stirring for 24 h until the color of the solution became a clear reddish brown. It was then purified by a Sephadex G-25 column chromatography (5 × 100 cm^2) with an eluent of neutralized water. The remaining trace catalyst and Na^+ ions were completely removed in this process. To obtain a final Gd-metallofullerenol product of a narrow region of distribution of the hydroxyl number, the fraction (eluate) was collected in a time interval of only several minutes. The elemental analysis method was used to measure the number of hydroxyl groups. Due to the fact that a precise determination of hydroxyl number is important for the present study, a further measurement of the hydroxyl number was performed using common X-ray photoemission spectroscopy.

The electronic properties of $Gd@C_{82}(OH)_x$, $Gd@C_{82}$, Gd-DTPA, and Gd_2O_3 were comparably studied using synchrotron radiation XPS at the photoelectron station of Beijing Synchrotron Radiation Facility, the Chinese Academy of Sciences. Samples were deposited onto the high-purity platinum substrates to obtain thin films for the XPS measurements, which were carried out in an ultravacuum chamber with background pressures of ~8 × 10^{-10} and ~1 × 10^{-9} Torr. Before the measurement, the samples were placed into the sample chamber of a ~10^{-9} Torr ultrahigh vacuum long enough to remove the possibly absorbed air or solvent molecules. X-ray photoemission spectroscopies of metallofullerenol C 1s were used to determine the number of hydroxyl groups. The Gd 4d, C 1s, O 1s X-ray photoabsorptions were obtained by collecting the partial electron yield. The experimental resolution was estimated to be ~0.5 eV. To inspect the contamination, XPS survey scans on the sample surface were performed before and after each measurement.

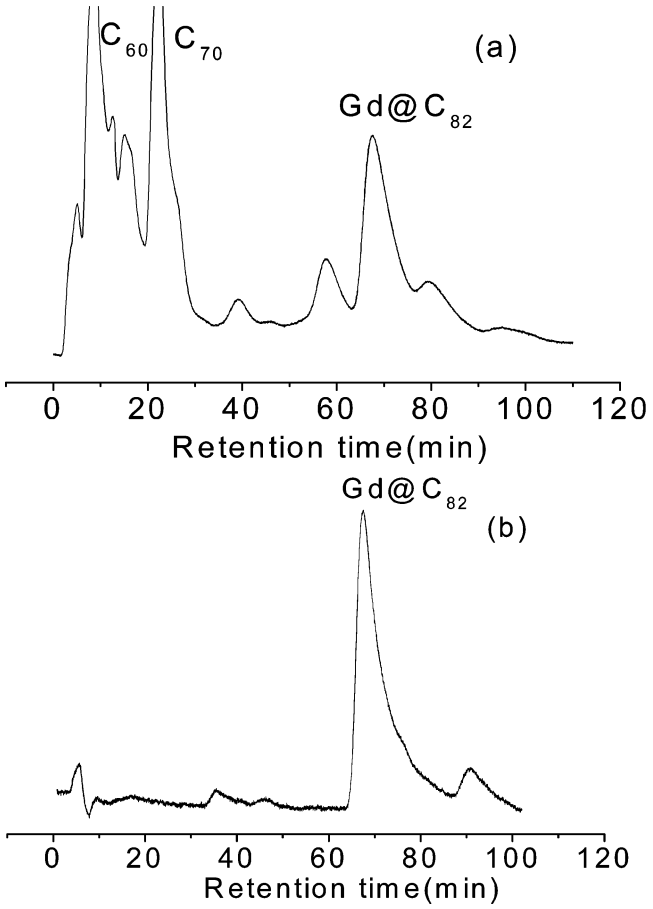

Figure 1. HPLC chromatograms for $Gd@C_{82}$ separated by 5PBB columns with 15 mL/min toluene as mobile phase (a), further isolation of $Gd@C_{82}$ by Buckyprep columns with 12 mL/min toluene (b).

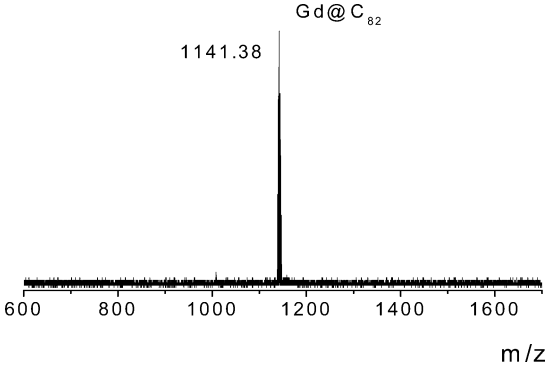

Figure 2. MALDI-TOF mass spectra of the HPLC-isolated $Gd@C_{82}$, positive ion and reflection modes.

Results and Discussion

Figure 1a shows the HPLC chromatographic spectra of the 5PBB column. The peak at about ~67.5 min corresponds to the species of $Gd@C_{82}$. Further isolation was carried out with Buckyprep columns, and the chromatogram is displayed in Figure 1b. The MALDI-TOF mass spectral analyses of the HPLC-isolated $Gd@C_{82}$ sample show a single peak at m/z = 1141.4 (Figure 2) in a wide mass region from m/z = 600 to 1700. $Gd@C_{82}$ with a high purity of greater than 99.9% was achieved. After the hydroxylation under different conditions, the element analysis (EA) showed that the hydroxyl number n

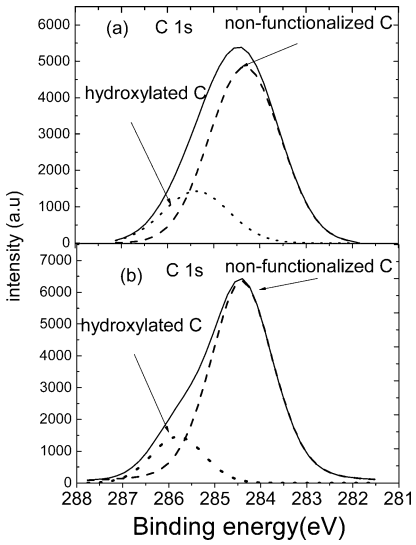

Figure 3. The XPS spectra for C 1s electrons in $Gd@C_{82}(OH)_{22}$ (a) and $Gd@C_{82}(OH)_{12}$ (b). The relative intensities between the C−C and C−O bonds were employed to determine the hydroxyl number in $Gd@C_{82}(OH)_x$.

of two $Gd@C_{82}(OH)_n$ samples was ∼24 and 13, respectively. However, EA is not a precise method for determining the hydroxyl number.[33] To obtain a more precise hydroxyl number, we used the X-ray photoemission spectroscopy to measure the binding energy spectra of C 1s electrons for C−C and C−O bonds in $Gd@C_{82}(OH)_n$ molecules, and a binary structure of C 1s XPS spectra was observed (Figure 3). For the pure component of C 1s electrons, the XPS spectrum is symmetric and well described by a true Voigt function with a Gaussian dispersion.[34] The Gaussian analysis of the solid lines in Figures 3 indicates the existence of two components: One centered at around 284.4 eV is the C 1s binding energies of sp^2 nonfunctionalized carbons (C−C); the other centered at around 285.3 eV is for hydroxylated carbons (C−OH). XPS spectra can differentiate the different carbons in the $Gd@C_{82}(OH)_n$ molecule, and this provides us with a more precise method to determine the hydroxyl number of $Gd@C_{82}(OH)_n$. Intensities of nonfunctionalized and hydroxylated carbons in $Gd@C_{82}(OH)_n$ were estimated from integration of the corresponding areas under the short line (I_{C-C} for C−C) and the dotted line (I_{C-O} for C−O) of Figure 3, respectively. As the total number of carbons is known to be 82, the number of hydroxylated carbons can hence be calculated from the related intensity I_{C-C} and I_{C-O} (being normalized to the total area under the solid line). I_{C-C} was found to be 73% and 85%, and I_{C-O} was found to be 27% and 15%, giving n to be ∼22 and ∼12 for samples a and b, respectively. They were smaller than the n values obtained from EA. Taking into account the ambiguity in both analysis methods, n was finally determined to be 22 ± 2 and 12 ± 2 for the metallofullerenols, and the chemical formulas for the two samples are $Gd@C_{82}(OH)_{22}$ and $Gd@C_{82}(OH)_{12}$, respectively.

Study of the electron−electron interactions along the chemical bonds from O of the outer-modified group to C of the cage surface, and finally to the innermost metallic atom Gd, may provide us with essential information about how much we can modulate the electronic properties of inner Gd through the chemical modifications of the outer cage. For this purpose, changes in the properties of the core level of O in $Gd@C_{82}(OH)_{22}$, $Gd@C_{82}(OH)_{12}$, and Gd_2O_3 were studied. The normalized absorption spectra of O 1s are shown in Figure 4a−c, respectively. Noting that there is no oxygen in the intact

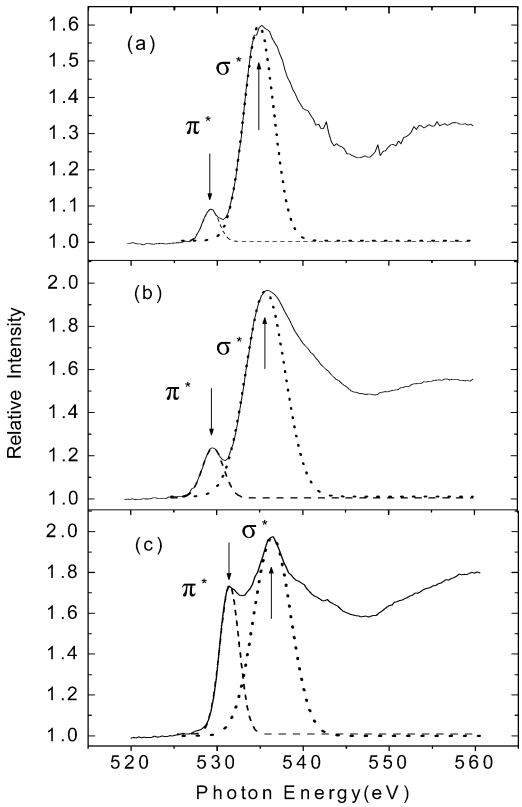

Figure 4. The O 1s absorption spectra of $Gd@C_{82}(OH)_{22}$ (a), $Gd@C_{82}(OH)_{12}$ (b), and Gd_2O_3 (c). The curves of solid and dotted lines are those obtained from the experiment and Gaussian analysis, respectively.

TABLE 1: Variations in Absorption Energy and Width of O 1s π^* and σ^* Electrons

	π^*		σ^*	
	peak (eV)	fwhm (eV)	peak (eV)	fwhm (eV)
$Gd@C_{82}(OH)_{22}$	529.3	1.9	534.9	3.5
$Gd@C_{82}(OH)_{12}$	529.6	2.4	535.7	4.6
Gd_2O_3	531.4	2.2	536.4	4.3

$Gd@C_{82}$, the variation of characteristics of bond electrons for O in hydroxyl-modified molecules ($Gd@C_{82}(OH)_x$) was hence studied using Gd_2O_3 as a reference. In Gd_2O_3, the intensity for π^* is comparable to that for σ^*, but the π^* peak is much weaker than the σ^* peak in either $Gd@C_{82}(OH)_{12}$ or $Gd@C_{82}(OH)_{22}$. The intensity and peak positions for σ^* absorption vary in sequence of $Gd@C_{82}(OH)_{22}$, $Gd@C_{82}(OH)_{12}$, and Gd_2O_3. Gaussian analysis was applied for distributions of σ^* and π^* absorptions. The analysis was done with initial parameters being completely free. The fitting process was performed by searching a Gaussian distribution, which can mostly fit the observed curve of the left side without linear overlap for the peak until the baselines of the peaks were consistent. The results are summarized in Table 1. The peak positions and full width at the half-maximum (fwhm) for both σ^* and π^* absorptions exhibit an orderly variation in sequence of $Gd@C_{82}(OH)_{22}$, $Gd@C_{82}(OH)_{12}$, and Gd_2O_3. For instance, π^* appears at about 529.3, 529.6, and 531.4 eV with a fwhm of 1.9, 2.4, and 2.2 eV, while σ^* appears at about 534.9, 535.7, and 536.4 eV with a fwhm of 3.5, 4.6, and 4.3 eV for $Gd@C_{82}(OH)_{22}$, $Gd@C_{82}(OH)_{12}$, and Gd_2O_3, respectively. The spectra of O absorptions demonstrated the presence of hydroxyl groups in samples a and b.

The π^* absorption becomes narrower from $Gd@C_{82}(OH)_{12}$ to $Gd@C_{82}(OH)_{22}$, indicating that the former has a lower degree

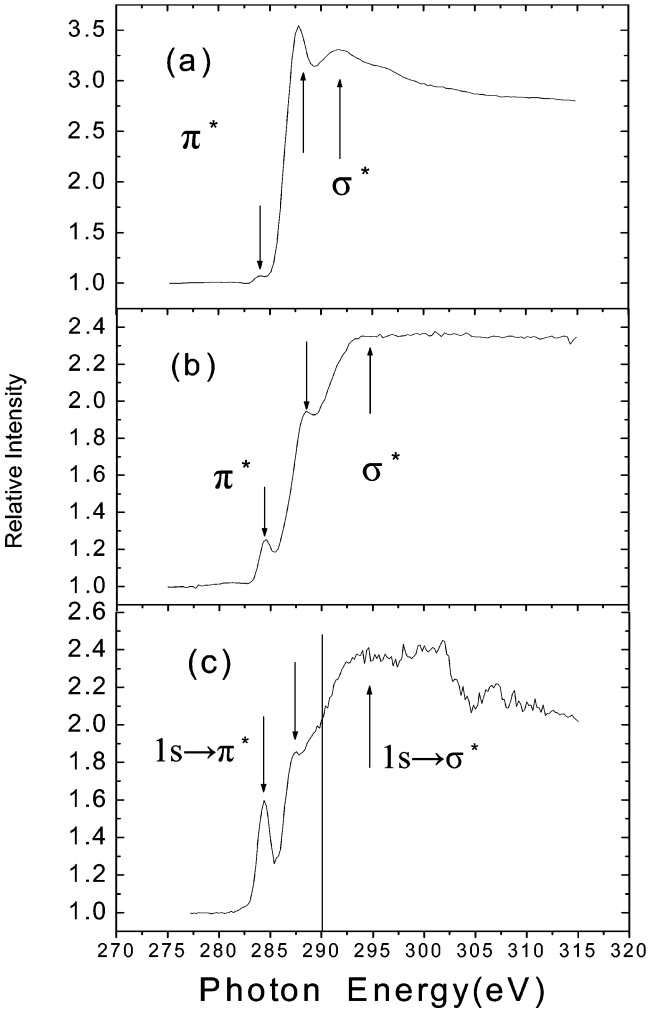

Figure 5. The C 1s absorption spectra of $Gd@C_{82}(OH)_{22}$ (a), $Gd@C_{82}(OH)_{12}$ (b), and $Gd@C_{82}$ (c). The absorption features from 284 to 290 eV correspond to 1s→π* transitions, while those above 290 eV correspond to 1s→σ* transitions.

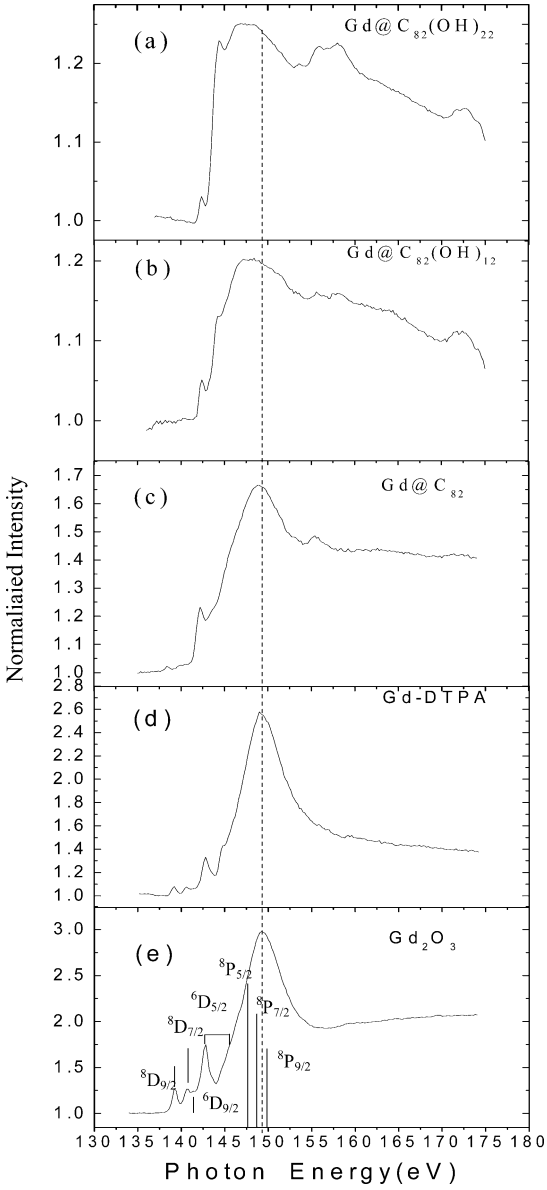

Figure 6. The Gd 4d→4f transitions spectra for $Gd@C_{82}(OH)_{22}$ (a), $Gd@C_{82}(OH)_{22}$ (b), $Gd@C_{82}$ (c), Gd-DTPA (d), and Gd_2O_3 (e). The vertically dotted line is drawn to guide the eyes to see the shift in the resonance peaks between the various Gd@fullerene molecules.

of degeneracy (density-of-state) of unoccupied molecular orbital states. Except for the change in energy levels caused by the chemical modifications, it may also be attributed to the existence of more options of reactive sites for a smaller number of hydroxyl groups. This easily increases the occurrence of random selection of the reaction sites for hydroxyl groups, leading to the possible presence of structural isomers and lowering the symmetry of the modified products.

The absorption spectra of the C K-edge are shown in Figure 5, in which the data were normalized by baseline. The absorption features from 284 to 290 eV correspond to 1s→π* transitions, while those above 290 eV correspond to 1s→σ* transitions. The binary structures rooted in level split were clearly observed at 284.4 and 287.8 eV in the 1s→π* transition region, providing detailed information regarding the electron transition process of the lowest level. The peak energies observed in Figures 5 are in good agreement with those reported by Suenaga et al.[35] and Pagliara et al.[36] In the process of 1s→π* transition, the relative intensity of the first peak of the energy split (284.4 eV) was lowered, while that of the second peak of the split (287.8 eV) became more intense from the intact $Gd@C_{82}$ to $Gd@C_{82}(OH)_{12}$ and finally to $Gd@C_{82}(OH)_{22}$. Similar phenomena were previously found in the fluoridation process of benzene.[37] These results suggest that the charge transfer between the modified groups and the cage can be largely altered when the outer cage of $Gd@C_{82}$ is differently modified, for instance, by a different number of hydroxyl groups. Thus, it educes an intriguing question: will this electronic interaction between the cage and outer modified groups influence the electronic properties of the innermost atom inside the nanospace of the cage? To this end, one needs to study the variation in electronic properties of Gd with the change of outer modifications. The photoabsorption spectra (normalized to the baseline) of Gd 4d for $Gd@C_{82}(OH)_{22}$, $Gd@C_{82}(OH)_{12}$, $Gd@C_{82}$, Gd-DTPA, and Gd_2O_3 are shown in Figure 6a−e, respectively. The X-ray absorption spectrum collected at the Gd 4d→4f edge is usually divided into pre-edge and resonance regions, as those observed in Figure 6d and e. The quantified results are listed in Table 2, showing variations in peak energy of the pre-edge and resonance absorption regions of Gd 4d→4f transition processes for the differently modified Gd-fullerenol molecules. The narrow pre-edge peaks are ascribed to the ^8D_J ($^8D_{9/2}$, $^8D_{7/2}$) and ^6D_J ($^6D_{9/2}$, $^6D_{5/2}$) multiplets, whereas the giant resonance is mainly ascribed to the ^8P_J ($J = {}^5/_2, {}^7/_2, {}^9/_2$) multiplets.[27,36] When metallic atom

TABLE 2: Variations in Energies of Pre-Edge and Resonance Regions of Gd 4d→4f Transition Processes

	peak position (eV)				
	$^8D_{9/2}$	$^8D_{7/2}$	$^6D_{5/2}$ (first split)	$^6D_{5/2}$ (second split)	resonant peak
$Gd@C_{82}(OH)_{22}$			142.4	144.4	147.4
$Gd@C_{82}(OH)_{12}$			142.4	144.4	147.2
$Gd@C_{82}$			142.2	144.2	148.8
Gd-DTPA	139.2	140.6	142.8	144.8	149.0
Gd_2O_3	139.2	140.8	142.8		149.2

is not astricted by the definite nanospace, absorption features of Gd 4d→4f are very similar for Gd metal[25] and different chemical compounds. For instance, few changes were observed for Gd_2O_3 (Figure 6e) and Gd-DTPA (Figure 6d). Yet the evident changes in the pre-edge region for Gd_2O_3 (Figure 6e) and $Gd@C_{82}$ (Figure 6c), in the resonance region for $Gd@C_{82}$, $Gd@C_{82}(OH)_{12}$, and $Gd@C_{82}(OH)_{22}$, and even behind the resonance region were observed, because of the different oxidation state of Gd metal. These suggest that when Gd atom was encaged by the nanospace of the fullerene cage, its 4d absorption spectra will change with the change of outer modifications.

The variation of fine structures observed in the pre-edge region, with the variation of different chemical modifications, is first considered. To explore the influence of chemical surroundings around Gd atom on the absorption process of Gd 4d→4f, XAS of a common compound Gd_2O_3 and a chelate compound Gd-DTPA served as the references and were studied together with the encaged Gd (in $Gd@C_{82}(OH)_x$). In Gd_2O_3, the $^6D_{5/2}$ level did not split (Figure 6e). Yet when Gd atom is semi-closed by the chelate in Gd-DTPA, its $^6D_{5/2}$ splits into two peaks (Figure 6d). This $^6D_{5/2}$ level splitting is largely enhanced when Gd is completely closed by a nanospace of C_{82} cage, in particular, when the cage is modified by the chemical groups of hydroxyl in $Gd@C_{82}(OH)_{12}$ and $Gd@C_{82}(OH)_{22}$. On the contrary, the intense absorptions of Gd $^8D_{9/2}$ and $^8D_{7/2}$ levels in Gd_2O_3 become weak as compared to Gd-DTPA. When Gd is completely encaged by a nanospace of C_{82} modified by hydroxyl, the absorptions of Gd $^8D_{9/2}$ and $^8D_{7/2}$ levels completely disappear. They are more clearly seen from the data in Table 2, the shift of peak energy of the pre-edge and resonance absorption for Gd 4d→4f transition processes of the differently modified Gd-fullerenols. Figure 7 shows the quantified results, presenting the changing tendency in the intensity of $^6D_{5/2}$ (a, the first level split), $^6D_{5/2}$ (b, the second level split), and the resonance peak (c) for various Gd-fullerenols $Gd@C_{82}$, $Gd@C_{82}(OH)_{12}$, and $Gd@C_{82}(OH)_{22}$, with those for the reference materials of Gd_2O_3 and Gd-DTPA. The results suggest that the intensity of electronic interactions between innermost Gd and carbon cages is altered by the outer modified chemical groups.

When Gd is encapsulated in the nanospace of C_{82}, the charge distribution of its 4d orbit electrons partially overlaps with the outer cage.[38] The C−C bond of the outer cage donates its charge back to the 4d orbit of the innermost Gd. This process hence changes the occupancy states of $^8D_{9/2}$ and $^8D_{7/2}$ with the back-bonding charges. When further modification of hydroxyl groups is applied to the outer carbon cage, oxygen, because of its high electronegativity, looks as if it is able to attract electrons from carbon of the cage. Yet this would lead to an impossible structure with an outer electronic configuration of more than 8 electrons in oxygen (Figure 8a). O of the newly added hydroxyl cannot accept any extra electrons. On the contrary, oxygen can donate electrons toward the "π" orbital of the carbon cage, similar to what occurs in the phenol (Figure 8b). As the charge

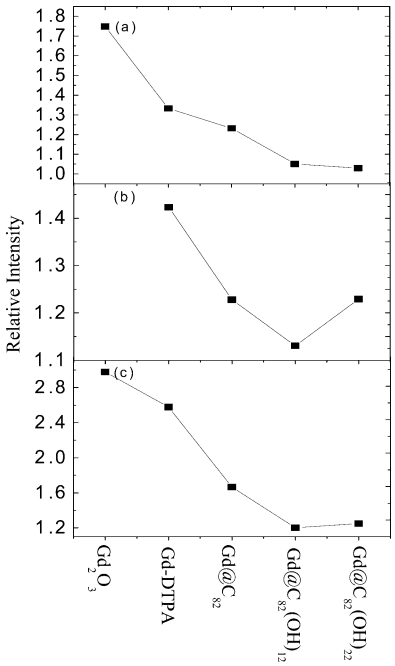

Figure 7. The changes in relative intensity of the first level split $^6D_{5/2}$ (a), the second level split $^6D_{5/2}$ (b), and the resonance peak (c), for Gd metal atom with different modifications in Gd_2O_3, Gd-DTPA, $Gd@C_{82}$, $Gd@C_{82}(OH)_{12}$, and $Gd@C_{82}(OH)_{22}$.

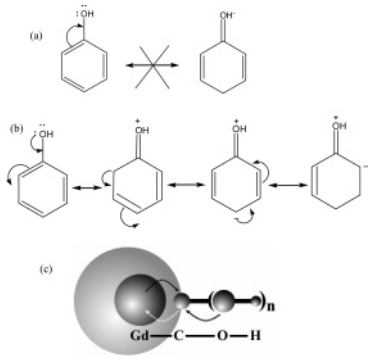

Figure 8. Schematic drawing of a sandwich-type electronic interaction pattern along [outer modification group]−[nano sheaths]−[inner metallic atom]. For details, see the text.

density distribution of carbon in the cage is partially overlapped with that of inner metallic atom, the effects of electronic interaction between outer oxygen and cage carbon can directly transfer to the inner Gd (Figure 8c). This process alters the fine structures of electronic configuration, as observed in Figures 6 and 7. For instance, for the level split of $^6D_{5/2}$, the intensity of the first split increases; meanwhile the second split decreases when the outer modification is altered by changing the number of hydroxyl groups.

In the resonance region of Figures 6, the dominant ^8P continuum mainly contains $^8P_{5/2}$,$^8P_{7/2}$, and $^8P_{9/2}$.[36] When Gd is not limited by a nanospace, as in Gd_2O_3 and Gd-DTPA, the giant resonance is dominated by the $^8P_{9/2}$ level and the contribution of $^8P_{5/2}$ is small, which makes a constricted absorption peak as observed in Figure 6d and e. As long as Gd is limited by the nanospace of C_{82}, the peak energy of giant resonance shifts from $^8P_{9/2}$ to the lower level $^8P_{7/2}$ in $Gd@C_{82}$ (Figure 6c). Because of the enhancement of resonance absorption at $^8P_{7/2}$, composition from $^8P_{9/2}$ and $^8P_{7/2}$ results in a broadened width as compared to that of Gd_2O_3 or Gd-DTPA. When the outer cage is chemically modified with hydroxyl, the

enhanced resonance absorption is changed at the energy level of $^8P_{5/2}$ in Gd@$C_{82}(OH)_{12}$ (Figure 6b) and Gd@$C_{82}(OH)_{22}$ (Figure 6a). Due to the similar reason that broadens the width of the resonance peak in Figure 6c, the resonance widths for both Gd@$C_{82}(OH)_{12}$ and Gd@$C_{82}(OH)_{22}$ are broadened.

The results suggest that less electrons are transferred from innermost Gd toward the π-orbital of Gd@$C_{82}(OH)_{22}$ (modified cage) than those toward the orbital of Gd@C_{82} (unmodified cage). This can be understood from schematically describing the process of electronic interactions, as shown in Figure 8c. As compared with the electron-transfer process in the unmodified Gd@C_{82}, the back-donation of electron from outer oxygen to carbon in Gd@$C_{82}(OH)_{22}$ lowered the electron-acceptability of the modified cage, which naturally restricts electrons transfer from Gd to the orbital of carbon cage. It is worthy noting that, in 1994, the theoretical calculation indicated that the electronic states of C_{82} endohedral lanthanoid atoms were unaffected by addition and removal of electrons to the cage.[39] In the current experiment, the charge transfer from the hydroxyl groups to the fullerene cage, which caused a change in the oxidation state of the innermost Gd, was observed. This difference between the early theoretical and presently experimental results may be attributed to the following reasons. The first is the quantitative differences in the number of electrons added to the cage: as compared to +2 in the calculations of the Ce atom, the charge in the experiment of Gd is larger than +2. The second is the different positions or motions between Gd and Ce[39] within the C_{82} cage, as revealed by the recent study.[38] The different position or motion of the metal atom inside the C_{82} leads to a different pattern of the electronic interactions between the innermost metal atom and carbon cage. For instance, in the calculation,[39] only fixed positions of metal atom along the C_2 axis were assumed and considered. For the GdC_{82} molecule, it has been recently found that Gd atom is locating in the vicinity of the C−C double bond with floating motions.[19,38] The third is that, in the early calculation, the metal atom donating its valency electrons to the cage was taken into account, but less considering the process of back-donation of electrons.[39] Further, to simplify the model, the interactions between core level of innermost metal atom and outer carbon cage were usually ignored,[20,39] but it has been recently demonstrated that these cannot be neglected.[38]

As far as the region behind the resonance was concerned, as compared to Gd_2O_3 and Gd-DTPA, a single peak was observed at 155.4 eV in Gd@C_{82}. While binary structures were resolved at ~155.8 eV, new peaks at 172 eV were observed in Gd@$C_{82}(OH)_x$ (Gd@$C_{82}(OH)_{22}$ and Gd@$C_{82}(OH)_{12}$). These results suggest that the processes of Gd-encapsulation and hydroxylation may result in new vacant states. When Gd atom is inserted into C_{82} cage, the 5p level is combined with cage electrons and then partly donates its 5p electrons to the cage. This not only causes the formation of a new vacant state, but also further causes the 4d→5p absorption structure to be observed. With the further hydroxylation, Gd 5p and 5s levels will more considerably mix with cage (Figure 6a,b) and will lead to more intense 4d→5p and 4d→5s absorption in sequence of Gd@C_{82}, Gd@$C_{82}(OH)_{12}$, and Gd@$C_{82}(OH)_{22}$. On the other hand, as the 5s and 5p electrons bond to the cage, it would make C_{82} back-donate more electrons to the Gd 4d level.

Conclusion

Metallic atom (gadolinium) was encapsulated by a definite nanospace of a fullerene cage using the arc-discharge method. After HPLC chromatographic separation by 5PBB and further isolation by Buckyprep columns, Gd@C_{82} (>99.9%) was chemically modified to be Gd@$C_{82}(OH)_{22}$ and Gd@$C_{82}(OH)_{12}$. After purification and a series of characterization using MALDI-TOF-MS, HPLC, common XPS, and element analysis, electronic properties of Gd_2O_3, Gd-DTPA, Gd@C_{82}, Gd@$C_{82}(OH)_{12}$, and Gd@$C_{82}(OH)_{22}$ were analyzed using synchrotron radiation X-ray photoemission spectroscopic techniques.

Level splits were clearly observed at 284.4 and 287.8 eV in the 1s→π* transition region of C 1s absorption spectra. The relative intensity of two split peaks is evidently changed with the change of modified groups, indicating that the charge transfer between the orbital electrons of cage (nano sheath) and inner Gd is changing with the change of the number of modified groups.

This was further demonstrated from the results of photoabsorption of the Gd 4d→4f transition. In the pre-edge region of the Gd 4d→4f transition, ^8D_J ($^8D_{9/2}$, $^8D_{7/2}$) and ^6D_J ($^6D_{9/2}$, $^6D_{5/2}$) multiplets evidently vary in sequence of Gd@$C_{82}(OH)_{22}$, Gd@$C_{82}(OH)_{12}$, Gd@C_{82}, Gd-DTPA, and Gd_2O_3. For instance, the $^6D_{5/2}$ energy level did not split in Gd_2O_3, but begins to split when Gd is semi-closed by the chelate in Gd-DTPA. The split pattern is largely altered as Gd is completely closed by a nanospace of C_{82} cage, in particular, when the cage is further modified by hydroxyl. On the contrary, the strong absorptions of Gd $^8D_{9/2}$ and $^8D_{7/2}$ levels in Gd_2O_3 become much weaker in Gd-DTPA and further disappear in Gd@$C_{82}(OH)_{12}$ and Gd@$C_{82}(OH)_{22}$. In the giant resonance region, ^8P_J ($J = {}^5/_2, {}^7/_2, {}^9/_2$) multiplets are observed with the peak positions moved to the lower energy side for Gd_2O_3, Gd@C_{82}, and Gd@$C_{82}(OH)_{12}$ to Gd@$C_{82}(OH)_{22}$. In Gd_2O_3 or Gd-DTPA, the resonance is dominated by $^8P_{9/2}$ level and the contributions of $^8P_{7/2}$ and $^8P_{5/2}$ are small. In Gd@C_{82}, $^8P_{7/2}$ is enhanced, resulting in a broadened resonance width. In Gd@$C_{82}(OH)_{12}$ and Gd@$C_{82}(OH)_{22}$, the enhanced resonance absorption further shifts to the $^8P_{5/2}$ level.

Absorption of oxygen π* orbital electrons appears at about 529.3, 529.6, and 531.4 eV with a fwhm of 1.9, 2.4, and 2.2 eV, while that of σ* appears at about 534.9, 535.7, and 536.4 eV with a fwhm of 3.5, 4.6, and 4.3 eV for Gd@$C_{82}(OH)_{22}$, Gd@$C_{82}(OH)_{12}$, and Gd_2O_3, respectively. This systematic variation with altering outer modifications is consistent with the results observed from C 1s→π* and Gd 4d→4f transitions. Outer modification of the carbon cage by hydroxylation creates a new structure behind the resonance region in Gd@$C_{82}(OH)_{12}$ and Gd@$C_{82}(OH)_{22}$ and results in a back-donation of more electrons from nanocage to the 4d level of the innermost Gd atom. The results indicate that through chemical modifications, changing numbers, or categories of modified groups, it is practicable to modulate the fine structures of electronic configurations of metallic atoms that are circumscribed by a nanospace.

Acknowledgment. We are grateful to Prof. Long Wei and Dr Chuangxin Ma of IHEP for preparing the film of XPS samples using the ultrahigh vacuum chamber of molecular spattering. Y.Z. acknowledges the funding support from the Chinese National Natural Science Foundation (10490180), the Ministry of Science and Technology (2001CCA3800), the National Center for Nanoscience and Nanotechnology (90406024), and a major project of the Chinese Academy of Sciences. K.I. acknowledges the funding support from the Chinese National Natural Science Foundation. A portion of the experiments described was carried out at the Beijing Synchrotron Radiation Facility.

References and Notes

(1) Beyers, R.; Kiang, C.-H.; Johnson, R. D.; Salem, J. R.; de Vries, M. S.; Yannoni, C. S.; Bethune, D. S.; Dorn, H. C.; Burbank, P.; Harich, K.; Stevenson, S. *Nature* **1994**, *370*, 196.

(2) Chai, Y.; Guo, T.; Jin, C.; Haufler, R. E.; Chibante, L. P. F.; Fure, J.; Wang, L.; Alford, J. M.; Smalley, R. E. *J. Phys. Chem.* **1991**, *95*, 7564.

(3) Alvarez, M. M.; Gillan, E. G.; Holczer, K.; Kaner, R. B.; Min, K. S.; Whetten, R. L. *J. Phys. Chem.* **1991**, *95*, 10561.

(4) Takata, M.; Nishibori, E.; Sakata, M.; Inakuma, M.; Yamamoto, Y.; Shinohara, H. *Phys. Rev. Lett.* **1999**, *83*, 2214.

(5) Hino, S.; Takahashi, H.; Iwasaki, K.; Matsumoto, K.; Miyazaki, T.; Hasegawa, S.; Kikuchi, K.; Achiba, Y. *Phys. Rev. Lett.* **1993**, *71*, 4261.

(6) Kessler, B.; Bringer, A.; Cramm, S.; Schlebusch, C.; Eberhardt, W.; Susuki, S.; Achiba, Y.; Esch, F.; Barnaba, M.; Cocco, D. *Phys. Rev. Lett.* **1997**, *79*, 2289.

(7) Pichler, T.; Golden, M. S.; Knupfer, M.; Fink, J.; Kirbach, U.; Kuran, P.; Dunsch, L. *Phys. Rev. Lett.* **1997**, *79*, 3026.

(8) Takahashi, T.; Ito, A.; Inakuma, M.; Shinohara, H. *Phys. Rev. B* **1995**, *52*, 13812.

(9) Hino, S.; Umishita, K.; Iwasaki, K.; Aoki, M.; Kobayashi, K.; Nagase, S.; John, T.; Dennis, S.; Nakane, T.; Shinohara, H. *Chem. Phys. Lett.* **2001**, *337*, 65.

(10) Hino, S.; Umishita, K.; Iwasaki, K.; Miyazaki, T.; Miyamae, T.; Kikuchi, K.; Achiba, Y. *Chem. Phys. Lett.* **1997**, *281*, 115.

(11) Maeda, Y.; Miyashita, J.; Hasegawa, T.; Wakahara, T.; Tsuchiya, T.; Feng, L.; Lian, Y. F.; Akasaka, T.; Kobayashi, K.; Nagase, S.; Kako, M.; Yamamoto, K.; Kadish, K. M. *J. Am. Chem. Soc.* **2005**, *127*, 2143.

(12) Furukawa, K.; Okubo, S.; Kato, H.; Shinohara, H.; Kato, H. *J. Phys. Chem. A* **2003**, *107*, 10933.

(13) Suzuki, S.; Kawata, S.; Shiromaru, H.; Yamauchi, K.; Kikuchi, K.; Kato, T.; Achiba, Y. *J. Phys. Chem.* **1992**, *96*, 7159.

(14) Johnson, R. D.; de Vries, M. S.; Salem, J.; Bethune, D. S.; Yannoni, C. S. *Nature* **1992**, *355*, 239.

(15) Nomura, M.; Nakao, Y.; Kikuchi, K.; Achiba, Y. *Physica B* **1995**, *208&209*, 539.

(16) Kikuchi, K.; Suzuki, S.; Nakao, Y.; Nakahara, N.; Wakabayashi, T.; Shiromaru, H.; Saito, I.; Ikemoto, I.; Achiba, Y. *Chem. Phys. Lett.* **1993**, *216*, 67.

(17) Xu, Z.; Nakane, T.; Shinohara, H. *J. Am. Chem. Soc.* **1996**, *118*, 11309.

(18) Takata, M.; Umeda, B.; Nishibori, E.; Sakata, M.; Saito, Y.; Ohno, M.; Shinohara, H. *Nature* **1995**, *377*, 46.

(19) Nishibori, E.; Iwata, K.; Sakata, M.; Takata, M.; Takata, H.; Kato, H.; Shinohara, H. *Phys. Rev. B* **2004**, *69*, 113412.

(20) Poirier, D. M.; Knupfer, M.; Weaver, J. H.; Andreoni, W.; Laasonen, K.; Parrinello, M.; Bethune, D. S.; Kikuchi, K.; Achiba, Y. *Phys. Rev. B* **1994**, *49*, 17403.

(21) Andreoni, W.; Curioni, A. *Phys. Rev. Lett.* **1996**, *77*, 834.

(22) Takata, M.; Nishibori, E.; Umeda, B.; Sakata, M.; Inakuma, M.; Shinohara, H. *Chem. Phys. Lett.* **1998**, *298*, 79.

(23) Zhao, Y. L.; Chen, Z. L.; Yuan, H.; Gao, X. F.; Qu, L.; Chai, Z. F.; Xing, G. M.; Yoshimoto, S.; Tsutsumi, E.; Itaya, K. *J. Am. Chem. Soc.* **2004**, *126*, 11134.

(24) Gerken, F.; Barth, J.; Kunz, C. *Phys. Rev. Lett.* **1981**, *47*, 993.

(25) Richter, M.; Meyer, M.; Pahler, M.; Prescher, T.; Raven, E. V.; Sontag, B.; Wezel, H.-E. *Phys. Rev. A* **1989**, *40*, 7007.

(26) Mishra, S. R.; Cummins, T. R.; Waddill, G. D.; Gammon, W. J.; van der Laan, G.; Goodman, K. W.; Tobin, J. G. *Phys. Rev. Lett.* **1998**, *81*, 1306.

(27) Starke, K.; Navas, E.; Arenholz, E.; Hu, Z.; Baumgarten, L.; van der Laan, G.; Chen, C. T.; Kaindl, G. *Phys. Rev. B* **1997**, *55*, 2672.

(28) Huang, H. J.; Yang, S. H. *Chem. Mater.* **2000**, *12*, 2715.

(29) Sun, B. Y.; Feng, L.; Shi, Z. J.; Gu, Z. N. *Carbon* **2002**, *40*, 1591.

(30) Kareev, I. E.; Bubnov, V. P.; Laukjina, E. E.; Koltover, V. K.; YagubsKii, E. B. *Carbon* **2003**, *41*, 1375.

(31) Ros, D. T.; Prato, M. *Chem. Commun.* **1999**, 663.

(32) Mikawa, M.; Kato, H.; Okumura, M.; Narazaki, M.; Kanazawa, Y.; Miwa, N.; Shinohara, H. *Bioconjugate Chem.* **2001**, *12*, 510.

(33) Xing, G. M.; Zhang, J.; Zhao, Y. L.; Tang, J.; Zhang, B.; Gao, X. F.; Yuan, H.; Qu, L.; Cao, W. B.; Chai, Z. F.; Ibrahim, K.; Su, R. *J. Phys. Chem. B* **2004**, *108*, 11473.

(34) Leiro, J. A.; Heinonen, M. H.; Laiho, T.; Batirev, I. G. *J. Electron Spectrosc. Relat. Phenom.* **2003**, *128*, 205.

(35) Suenaga, K.; Iijima, S.; Kato, H.; Shinohara, H. *Phys. Rev. B* **2000**, *62*, 1627.

(36) Pagliara, S.; Sangaletti, L.; Cepek, C.; Bondino, F.; Larciprete, R.; Goldoni, A. *Phys. Rev. B* **2004**, *70*, 035420.

(37) Hitchcock, A. P.; Fischer, P.; Cedanken, A.; Robin, M. B. *J. Phys. Chem.* **1987**, *91*, 531.

(38) Senapati, L.; Schrier, J.; Whaley, K. B. *Nano Lett.* **2004**, *4*, 2073.

(39) Nagase, S.; Kobayashi, K. *Chem. Phys. Lett.* **1994**, *228*, 106.